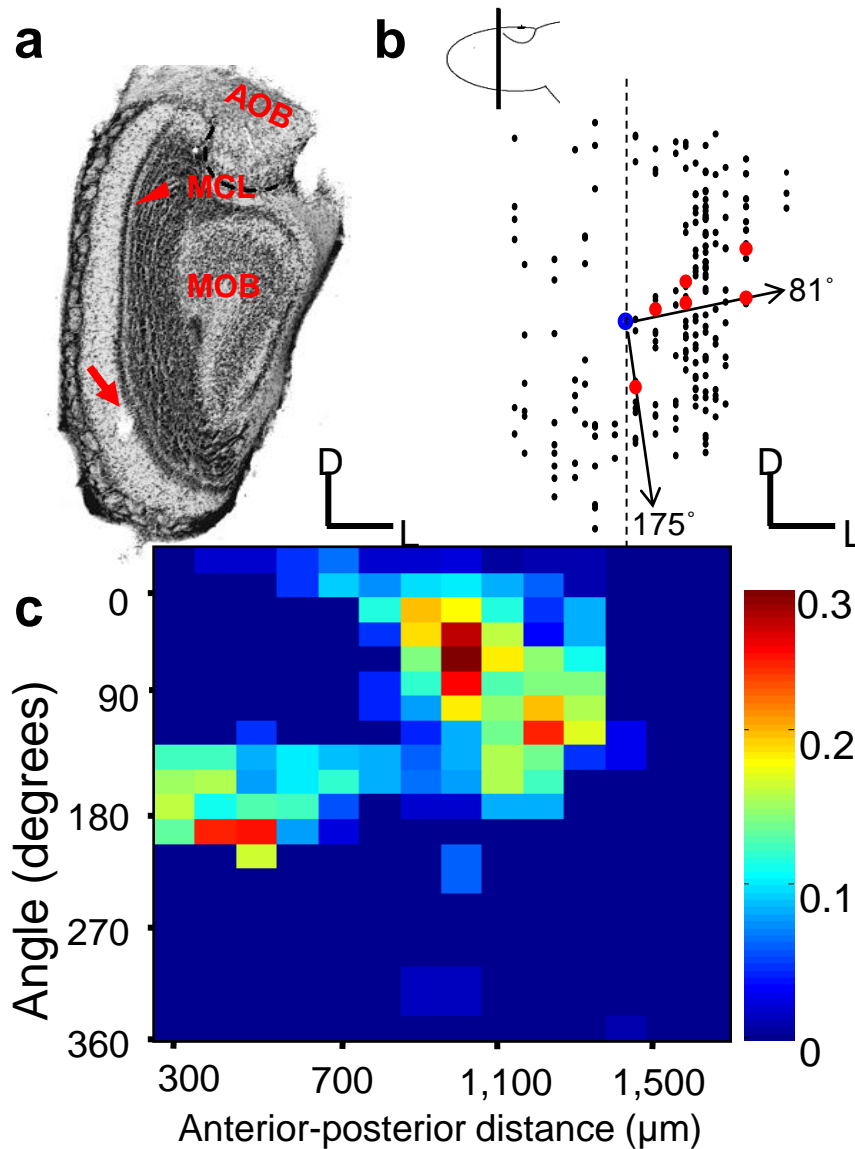


## **Supplemental information**

### **Encoding social signals in the mouse main olfactory bulb**

**Lin D, Zhang SZ, Block E, Katz LC.  
Nature. 434(7032):470-7**

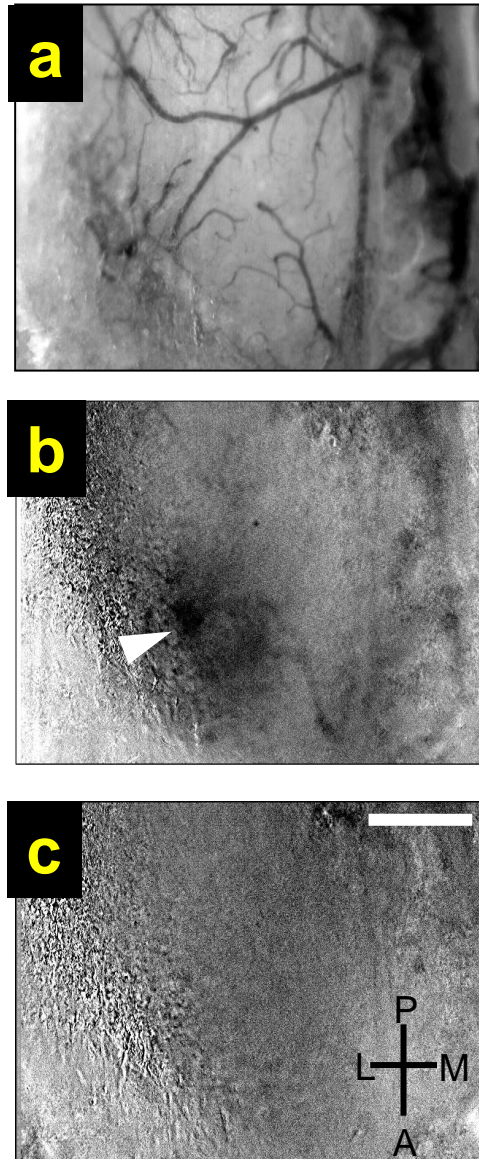
# Supplementary Fig. 1



**Supplementary Figure 1.** Clustered organization of urine responsive neurons in the main olfactory bulb. **A.** Verification of recording sites. Cresyl violet-stained coronal section showing an electrolytic lesion (red arrow) at the recording site of the mitral cell shown in Fig. A. This lesion is located in the ventro-lateral region of the bulb, 300  $\mu\text{m}$  anterior to the origin of the map. The origin is defined as the intersection of the sagittal suture and the major sinus separating the bulbs and the cortex (See Methods). Dashed line demarcates the border between the accessory olfactory bulb (AOB) and the main olfactory bulb (MOB). MCL, mitral cell layer. **B.** Clustering of urine responsive mitral cells in the ventral-lateral region of the olfactory bulb. Using their 3-dimensional stereotaxic coordinates, the positions of all cells recorded from female mice were plotted onto a single representative bulb. In a virtual 100  $\mu\text{m}$ -thick coronal slice taken through this composite MOB, the positions of all recorded cells

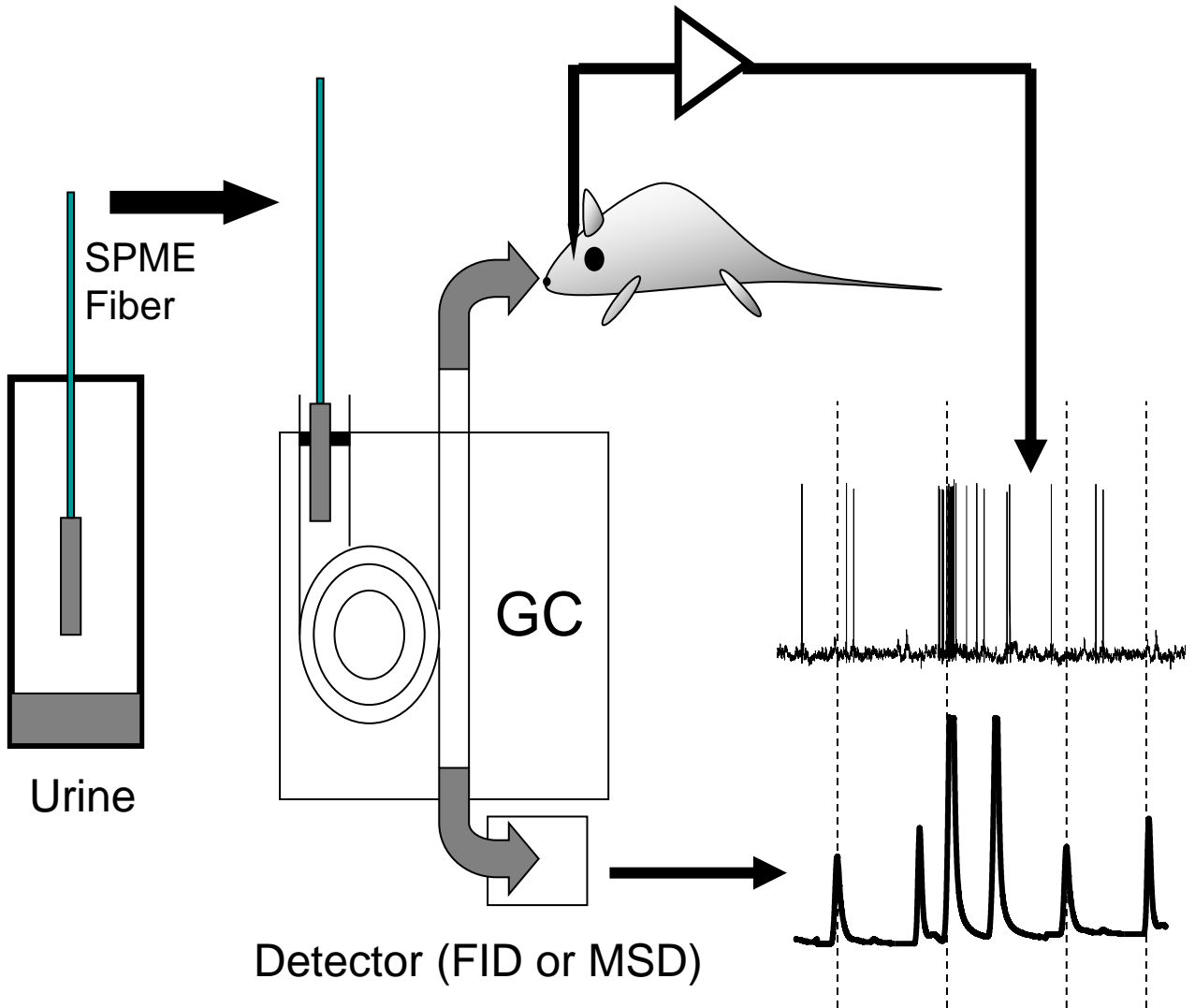
are indicated by *dots* (the position of the virtual slice, 900 -1000  $\mu\text{m}$  anterior to the origin, is indicated as a line on a sagittal view of the composite MOB). *Red dots* represent urine responsive cells. To construct a 2-dimensional representation of the probability of encountering a urine-responsive neuron at a given location (shown in **C**), coronal plots like this were created for all anterior-posterior positions. From the medial-lateral and dorsal-ventral midpoint of each section (blue dot), the angle of each cell's position was measured, with the dorsal surface representing  $0^\circ$  and the ventral pole  $180^\circ$ . The two responsive cells are located laterally ( $81^\circ$ ) and ventrally ( $175^\circ$ ). **C. Clustering of urine-responsive mitral cells in the olfactory bulb.** A pseudocolored probability index map (see Supplementary Methods) of all recorded neurons indicates that urine responsive neurons were encountered with highest probability in a lateral area located in the middle portion of the MOB and in a smaller zone located more posterior and medially. Anterior-posterior distances are calculated from the origin of the map. This analysis method is a modification of previous methods<sup>15</sup> used to construct 2-D *c-fos* expression maps. Color bar, probability value.

## Supplementary Fig. 2



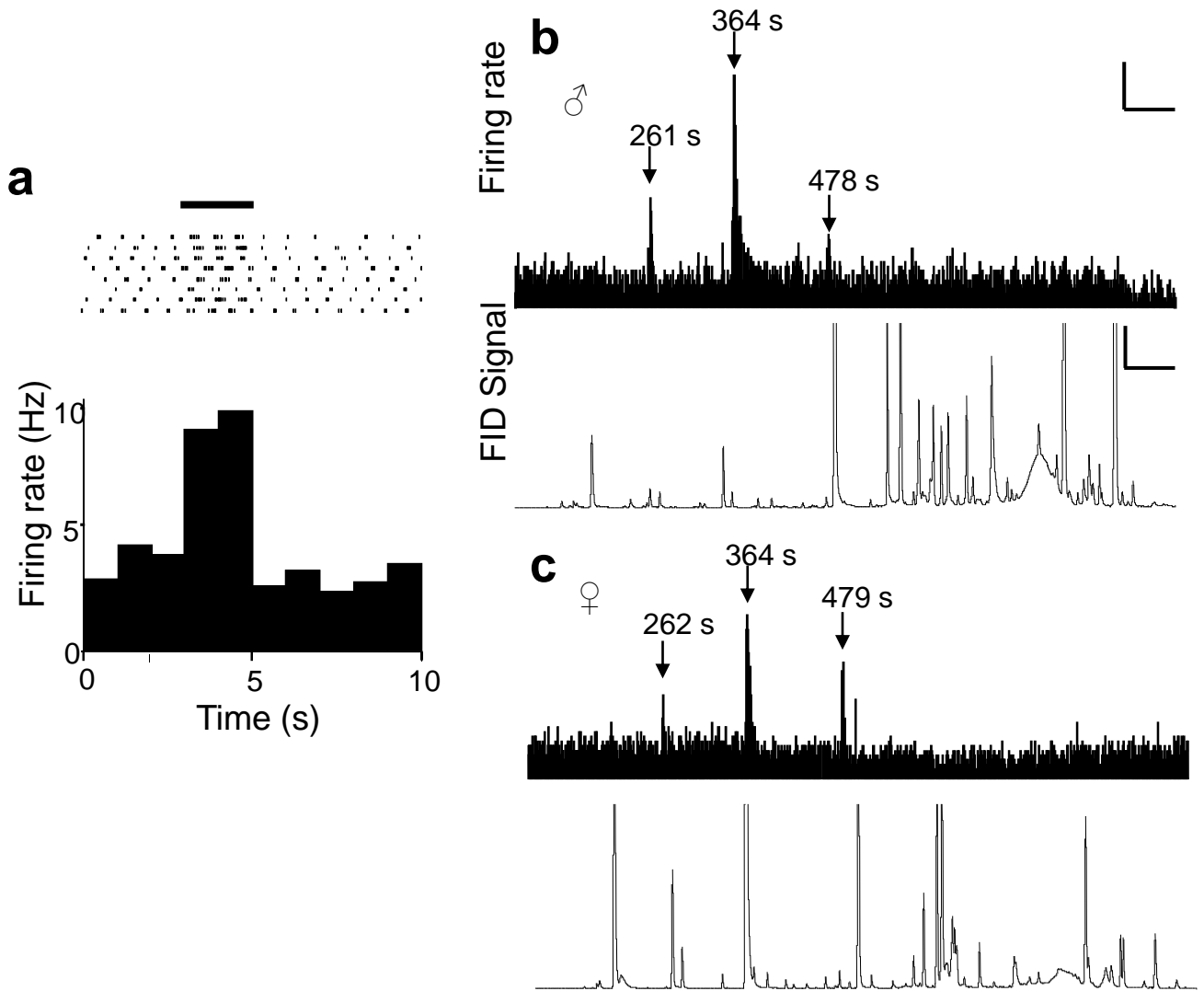
**Supplementary Figure 2.** Optical imaging of intrinsic signals reveals no glomerular activation in response to urine odor on dorsal surface of the MOB. **A.** Surface blood vessels overlying the imaged region. **B.** Butanal (0.1%) strongly activated several glomeruli in the antero-lateral region of the dorsal bulb. **C.** Volatile odorants from undiluted C57BL/6 male mouse urine failed to activate any glomeruli on the dorsal surface. Scale bar, 500  $\mu\text{m}$ .

## Supplementary Fig. 3



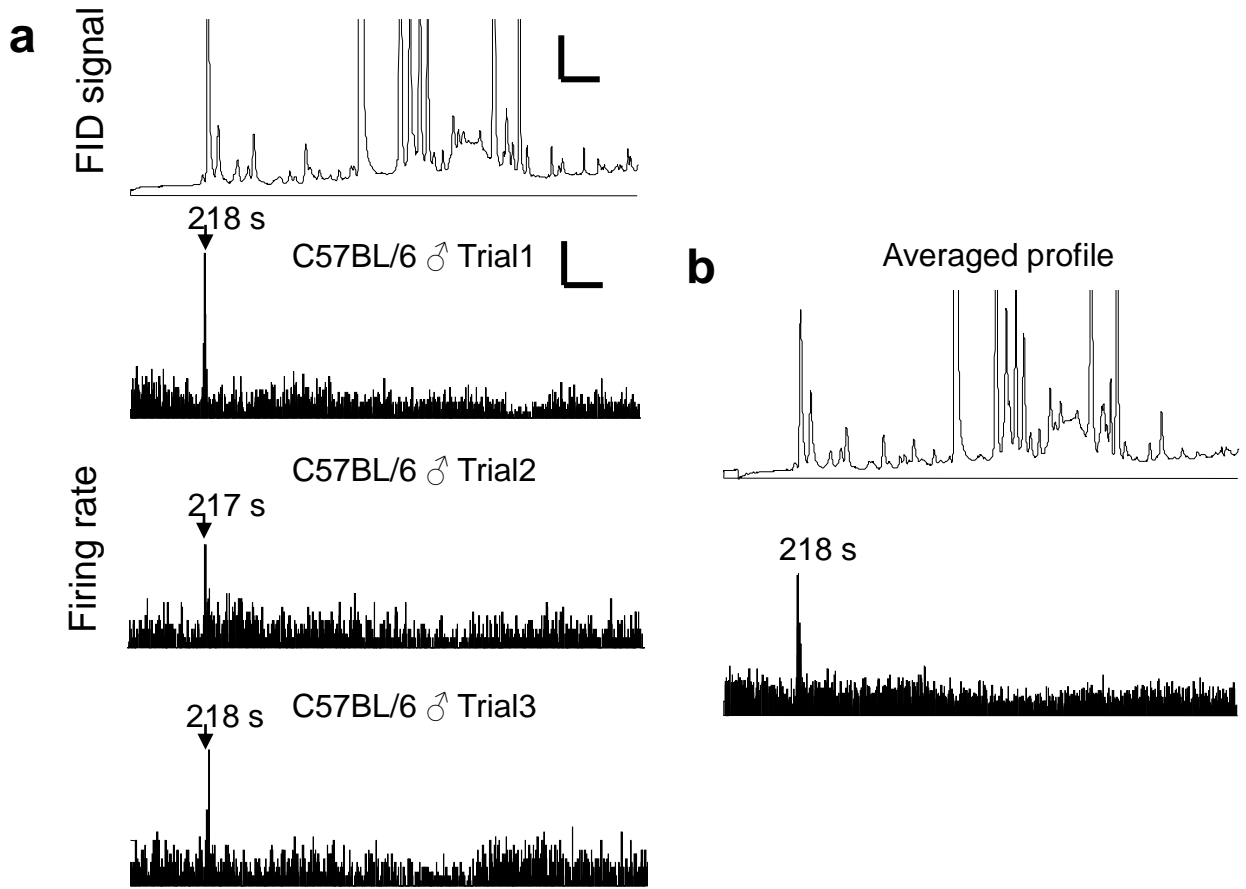
**Supplementary Figure 3.** Schematic representation of a gas chromatography-electrophysiology (GC-E) experiment. A solid phase microextraction (SPME) fiber is used to extract volatiles from the headspace above a sample of urine. Placing the SPME fiber in the heated injection port of the GC releases the adsorbed volatiles. Depending on the GC column used, individual components elute sequentially according to their boiling point (BP-5 column) or polarity (BP-20 column). The effluent from the column is split such that half of the flow enters either the GC's flame ionization detector, which ionizes compounds and produces a voltage signal, or a mass spectroscopy detector (MSD), which signals total ion abundance. The other half of the effluent is carried by a heated transfer line and arrives simultaneously at the animal's nostrils. Calibration of the system using known compounds demonstrated that there is < 1 s difference between the arrival of compounds at the GC detector and the nose. The extracellular spikes of a urine-responsive mitral cell are continuously recorded during the 20 minutes of odor delivery via GC.

# Supplementary Fig. 4



**Supplementary Figure 4.** Urine responsive cells activated by multiple compounds in urine. **A.** Raster plots and peristimulus time histogram of a neuron responsive to mouse urine volatiles (delivered during the time shown by the black bar). **B, C.** Two GC-E recordings from the cell in **A.** The upper panels show the firing rate of the cell corresponding to the gas chromatograms (lower panels) of C57BL/6 male mouse urine (**B**) and Balb/C female mouse urine (**C**) (Scales as in Fig. 2B, C). Arrows indicate the times when the cell was activated in these two independent GC-E recordings. In this case the cell was activated by molecules eluting at 3 distinct times, although the activation at 364 s was consistently larger than the other two.

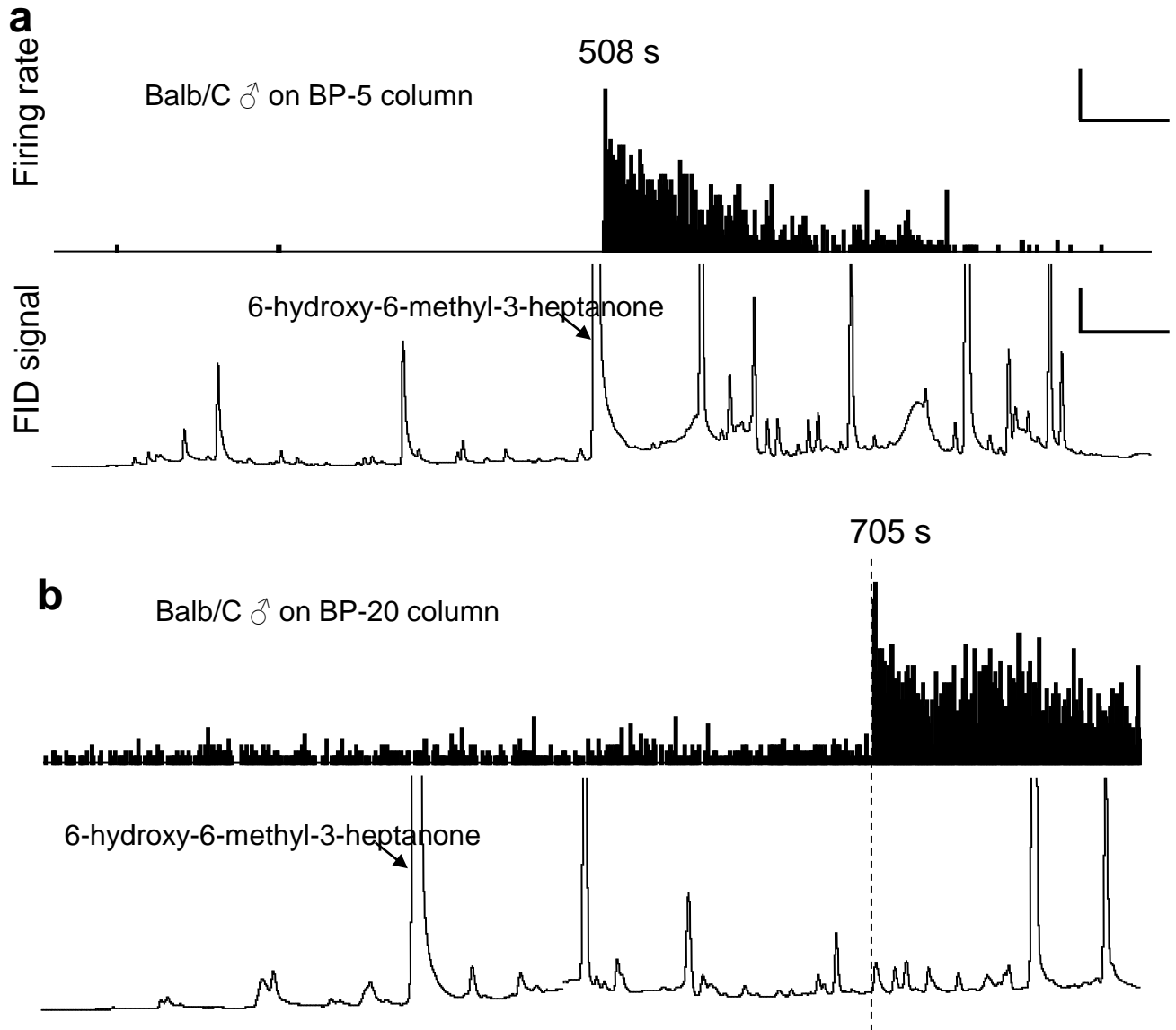
# Supplementary Fig. 5



**Supplementary Figure 5.** Averaging multiple GC runs does not reveal the presence of additional weak responses. **A.** A urine responsive cell's activity (shown in 1 sec bins) in three independent GC-E experiments (three lower panels) using C57BL/6 male mouse urine volatiles (upper panel) as stimuli (Scales as in Fig. 2B, C). The time point at which the cell was activated is indicated by black arrows. **B.** The averaged profile from data shown in **(A)** indicates that the cell was activated exclusively at one time point (218 s).

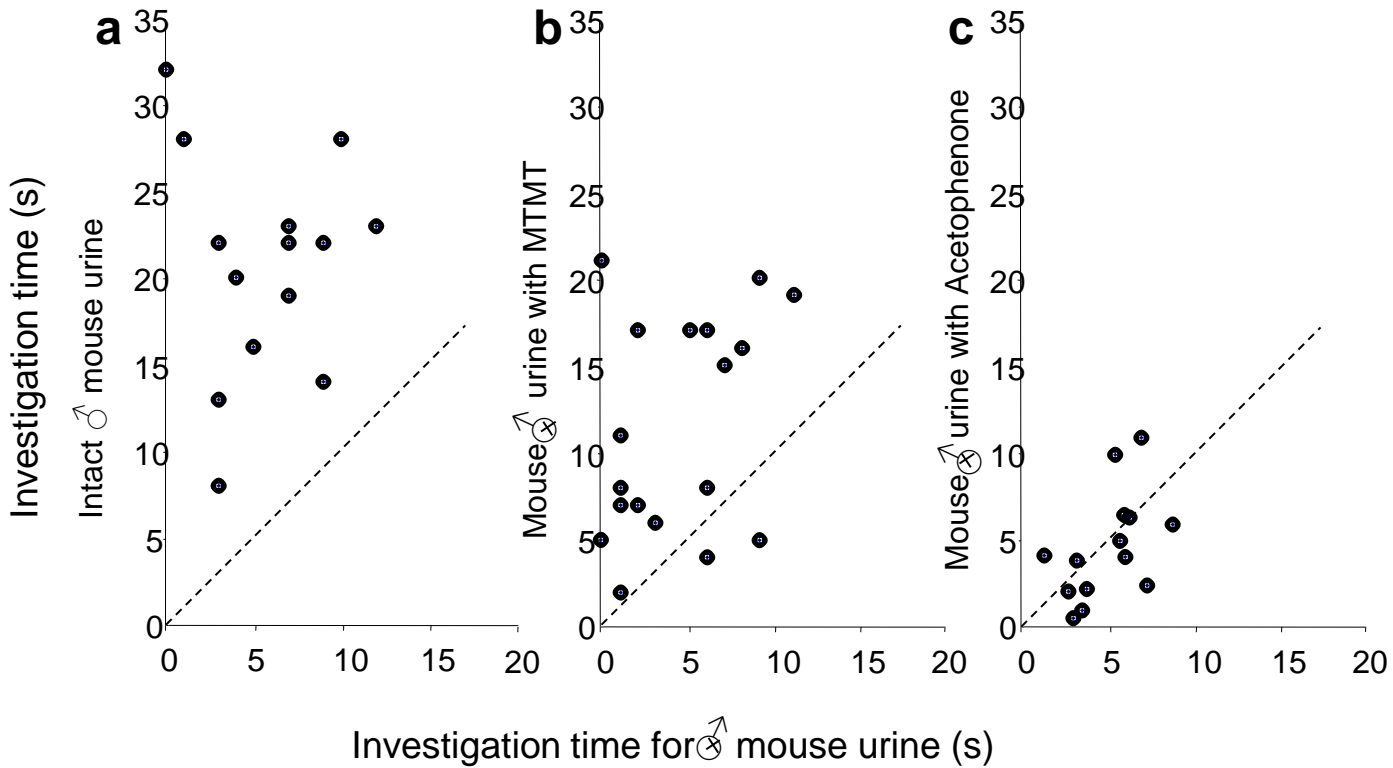


# Supplementary Fig. 7



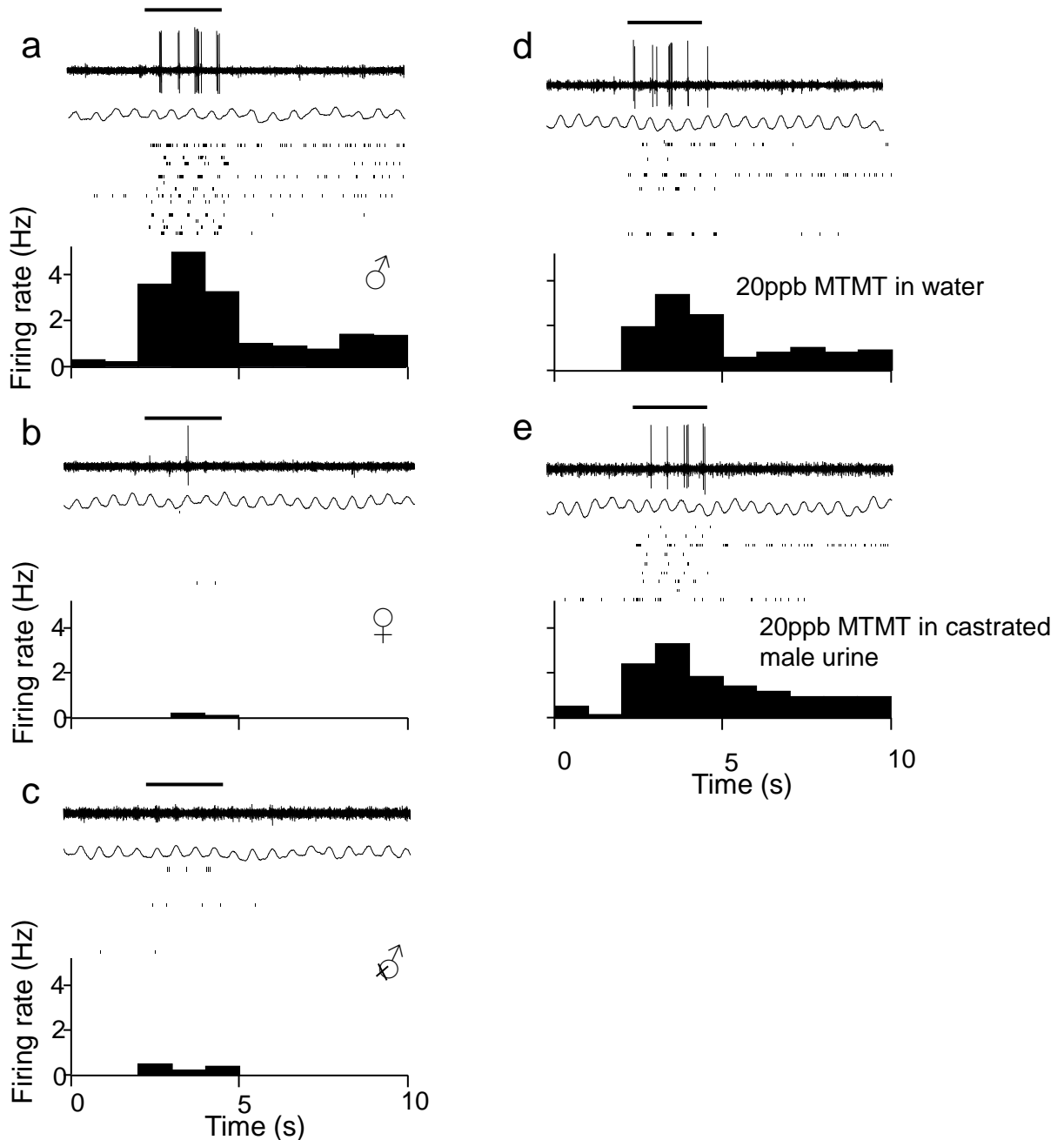
**Supplementary Figure 7.** The known pheromone 6-hydroxy-6-methyl-3-heptanone (6H6M3H) is not responsible for excitation of male-urine selective mitral cells. **A.** Separation of urine volatiles by boiling point (BP-5 column) revealed that a typical male specific cell was activated immediately following the elution of 6H6M3H. **B.** In a subsequent GC run, separating volatiles by polarity using a BP-20 column, this cell was excited at 705 s, far after elution of the 6H6M3H peak (indicated by the arrow) (Scales as in Fig. 2B, C).

## Supplementary Fig. 8



**Supplementary Figure 8.** Scatter plots comparing the investigation times for intact, castrated and MTMT-containing urine. **A.** All female mice tested spent more time investigating intact male mouse urine than castrated male mouse urine. **B.** All but two animals preferred MTMT spiked castrated male mouse urine to castrated urine alone. **C.** Adding exogenous acetophenone (1 ppm or 10 ppm) neither biased animals' choices nor increased their overall investigation time. Dashed line indicates equal time investigating each stimulus (i.e. no bias).

# Supplementary Fig. 9



**Supplementary Figure 9.** Neuronal responses elicited by MTMT are independent of other components in castrated mouse urine. **A-C.** Responses of a typical MTMT responsive mitral cell to stimulation by urine volatiles (2 s, indicated by black bar) from male mouse urine (**A**) female mouse urine (**B**) and castrated male mouse urine (**C**). An extracellular recording trace is shown, with the animal's breathing rhythm immediately beneath. Raster plots and post-stimulus time histograms show responses to multiple stimulus presentations. **D, E.** Volatiles from 20 ppb MTMT in water (**D**) or in castrated male mouse urine (**E**) caused similar cell responses.

## Supplementary Methods

### Constructing cell response map

To construct a map of responsive cell locations, the stereotaxic coordinates of all cells (both responsive and nonresponsive) were recorded (x: medial-lateral, y: posterior-anterior, z: dorsal-ventral). The position of each cell relative to the sagittal suture was used to assign medial lateral positions, and anterior positions were measured relative to the large sinus separating the bulbs from the cortex. Based on their distance anterior to this landmark, the 2734 recorded cells from all female mice were binned into five 400  $\mu\text{m}$  sections beginning at 300  $\mu\text{m}$  anterior to the landmark. The maximum and minimum recorded coordinates in the median-lateral and dorsal-ventral directions of the neurons assigned to each bin were used to calculate the center of that section. Linear curve fitting was performed on section centers to generate a centerline in the anterior-posterior direction (correlation coefficient = 0.94). Positions of recorded cells within each bin were then transformed into polar coordinates using this centerline to calculate corresponding origins. Cells were then arrayed into bins of  $18^\circ$  and 100  $\mu\text{m}$  based on their polar angles and posterior-anterior distances. The 0- $180^\circ$  axis is parallel to the z axis in Cartesian coordinates. The probability index for each bin was calculated as the ratio between the number of urine response cells at a given location and the total number of cells recorded at that location. These data were then smoothed using a 2 x 2 kernel to decrease errors caused by biological and mapping variability. The kernelled data were then visualized as a color map using a program written in Matlab 6.5.1.

### Synthesis of (methylthio)methanethiol

Thiourea (3.1 g, 40 mmol) was added to a solution of chloromethyl methyl sulfide (1.9 g, 20 mmol) in dry ethanol (30 mL). The mixture was refluxed for 48 h, concentrated in vacuo and the residue was dissolved in water (20 mL) and treated with NaOH solution (40%, 40 mL) for 15 minutes. The solution was then extracted with ether (2 × 30 mL). The combined ether extracts were then washed with brine (30 mL) and the solution was concentrated in vacuo yielding a colorless oil (1.2 g, 64% in yield, > 95% in purity) with a strong, pungent odor. Characterization by NMR yielded the following: <sup>1</sup>H NMR (300 MHz, CDCl<sub>3</sub>) δ 3.64 (d, J = 8 Hz, 2 H), 2.22 (s, 3H), 1.86 (t, J = 8 Hz, 1H); <sup>13</sup>C NMR (75 MHz, CDCl<sub>3</sub>) δ 30.2, 14.4. By GC-MS (in electron-ionization mode) the following values were obtained: m/z 94 (M<sup>+</sup>, 67%), 61 (49%), 45 (100%).